NORSAR Scientific Report No. 1-2010

Semiannual Technical Summary

1 July - 31 December 2009

Frode Ringdal (ed.)

Kjeller, February 2010

6.4 Location of the NDC Preparedness Exercise 2009 event with the use of near-regional data

6.4.1 Introduction

This contribution focuses on our efforts to relocate the NDC Preparedness Exercise 2009 (NPE09) event with the use of near-regional data. The starting information about the selected event, as received from the German NDC, is presented in Box 6.4.1.

Box 6.4.1. NPE09 event information as distributed via E-mail by the German NDC.

```
Event parameters from SEL3:

     EventID                        5727516
     Date                        2009/11/28
     Origin Time                07:20:31.21
     Epicenter     Latitude     50.1853° N
                   Longitude    77.4514° E
     Depth                           0.0 km
     Magnitude                       ML 3.4
     Region            Eastern Kazakhstan


The event was defined by two primary seismic stations at regional distances
and a primary station at PKP distance. It is also associated with a detection
at infrasound station I46RU. This event is included in the SEL1, SEL2, and
SEL3.

The closest operational radionuclide station is MNP45. The results of the
ATM forward modeling indicate that a signal from this event may be expected
about three days after origin time.
```

The issued Reviewed Event Bulletin (REB) solution of the International Data Centre (IDC) for the NPE09 event is presented in Box 6.4.2. In the REB the event is located in Eastern Kazakhstan, close to the Kara-Zhyra open mine, which is situated in the Balapan sector of the former Soviet Semipalatinsk Test Site (STS). According to information from Zlata Sinyova of the Kazakh NDC (KNDC), the event was the result of an open pit mining explosion, close to the border of the Western Kara-Zhyra mine. Complete ground truth information about the event is not available. However some characteristics of the ripple fired explosion are known and are listed below.

- Area equal to 10975 m^2
- Detonation at 171 boreholes with average depth of 13 m
- Boreholes arranged in 10 rows
- Delay time between detonations: 0.035 s
- Mass of explosive material (possibly Igdanit): 54193 kg

According to the KNDC, the Kara-Zhyra mine has the following geographic coordinates:

- Western Kara-Zhyra mine: 50.0183°N, 78.7265°E
- Eastern Kara-Zhyra mine: 50.0231°N, 78.7449°E

The mine is clearly visible in Google™ Earth where also the locations of known, past nuclear tests can be seen.

Box 6.4.2. The REB solution for the NPE09 event.

```
EVENT  5727516 EASTERN KAZAKHSTAN
   Date       Time        Err   RMS Latitude Longitude  Smaj  Smin  Az Depth   Err Ndef Nsta Gap
mdist  Mdist Qual   Author
 OrigID
2009/11/28 07:20:38.58   0.99  1.34  49.9622   78.7531  22.2   8.2  43   0.0f        9    4 162
3.95   6.06 m i uk IDC_REB
5736538

Magnitude  Err Nsta Author      OrigID
ML     3.1 0.2    3 IDC_REB    5736538
mb1    3.1 0.3    3 IDC_REB    5736538
mb1mx  3.0 0.2   30 IDC_REB    5736538
mbtmp  3.1 0.3    3 IDC_REB    5736538

Sta      Dist  EvAz Phase         Time       TRes  Azim AzRes   Slow   SRes Def   SNR        Amp
Per Qual Magnitude    ArrID
KURK    0.68 347.9 Pg       07:20:46.169  -5.9 152.9 -14.8   25.2    6.1 ___ 174.8       14.6
0.33 a__             55040383
KURK    0.68 347.9 Lg       07:20:57.504  -3.6 176.5   8.8   32.2   -1.7 ___  35.3       20.1
0.33  __             55160858
KURK    0.68 347.9 Rg       07:21:01.504  -2.1  97.6 -70.1   29.0   -8.1 ___  14.2       36.5
0.49  __             55160859
MKAR    3.95 142.0 Pn      07:21:40.650  -0.2 328.5   3.8   11.2   -2.5 TA_  39.7 0.9 0.33 a__
ML 2.9 55037946
mb1    2.9
mbtmp  2.9
MKAR    3.95 142.0 Pg       07:21:48.886   1.4 320.2  -4.4   14.1   -4.1 TA_  22.6        1.9
0.33  __             55141662
MKAR    3.95 142.0 Sn       07:22:31.068   3.5 322.2  -2.4   12.9  -11.8 ___   2.8        0.8
0.33  __             55141660
MKAR    3.95 142.0 Lg       07:22:43.496  -0.7 323.7  -1.0   27.3   -4.4 TA_  15.7        4.6
0.33  __             55141658
I46RU    5.48   40.9  I          07:50:10.000  -145.  220.6   -5.1   325.8   -24.2  _A_    2.9
a__           55038570
ZALV    5.48  40.9 Pn       07:22:00.975  -0.4 232.4   6.7   14.2    0.5 TA_  25.1        1.7
0.33 a__ ML     3.6 55037891
mb1    3.8
mbtmp  3.8
ZALV    5.48  40.9 Sn       07:23:22.313  16.2 228.1   2.4   20.9   -3.8 ___   4.3        0.2
0.33  __             55141659
ZALV    5.48  40.9 Lg       07:23:33.184   0.6 225.0  -0.7   28.7   -3.0 TA_   6.5        0.5
0.33 a__             55037892
BVAR    6.06 303.6 Pn       07:22:08.269  -0.2 120.2   3.1   14.0    0.3 TA_   3.6        0.3
0.33  __ ML     2.9 55141661
mb1    2.7
mbtmp  2.7
BVAR    6.06 303.6 Sn       07:23:16.107  -0.7 110.5  -6.6   22.4   -2.3 TA_  10.0        1.0
0.33 a__             55040591
BVAR    6.06 303.6 Lg       07:23:47.758  -3.3 116.4  -0.6   30.0   -1.8 TA_   6.0        0.7
0.33 a__             55040592
```

The IMS primary and auxiliary seismic stations within a 40° epicentral distance from the event can be seen in Fig. 6.4.1, copied from the NPE09 related web-page of the German NDC.

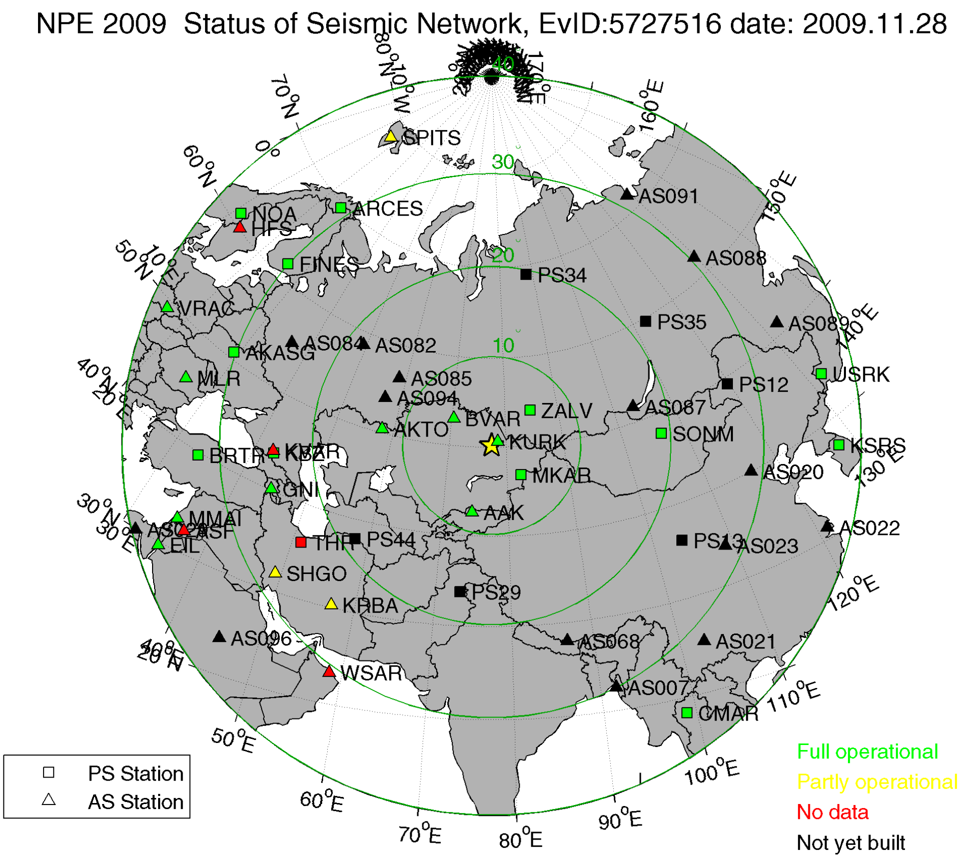

Fig. 6.4.1. Map of IMS primary (PS) and auxiliary (AS) seismic stations up to a distance of 40° from the selected NPE09 event (yellow star). From the NPE09 related web-page of the German NDC (http://www.seismologie.bgr.de/NPE).

6.4.2 Analysis and discussion

The REB solution

The REB NPE09 solution shown in Box 6.4.2 uses data from the seismic arrays Kurchatov (KURK), Makanchi (MKAR), Zalesovo (ZALV) and Borovoye (BVAR), and the infrasound station I46RU collocated with ZALV (for station locations see Fig. 6.4.1). A first inspection of the solution shows rather large residuals for certain stations, both for arrival times and backazimuth results. In order to look further into this matter, all available readings from the stations in the REB solution for events in the region since 01/01/2001 were retrieved, and the mean and median residuals for the entire dataset were compared to those reported in the REB NPE09 solution. The comparison results can be seen in the series of tables that follow (Tables 6.4.1 – 6.4.4). Except for the REB NPE09 and the mean ($_{me}$) and median ($_{md}$) residuals for each phase, the tables provide the number of observations (N) included in the retrieved dataset and which entry of the REB appears to be problematic (T - time, B - backazimuth, S - slowness, N - number).

Table 6.4.1. Comparison between REB entry for NPE09 and REB (2001 - 2009) mean and median onset time, backazimuth and slowness residuals for the KURK array.

phase	NPE09 Tres	REB $Tres_{me}$	REB $Tres_{md}$	NPE09 Bres	REB $Bres_{me}$	REB $Bres_{md}$	NPE09 Sres	REB $Sres_{me}$	REB $Sres_{md}$	REB N	NPE09 problematic
Pg	-5.9	0.1	-0.3	-14.8	0.7	1.2	6.1	-1.3	-1.1	67	TAS
Lg	-3.6	-2.8	-2.3	8.8	2.7	3.5	-1.7	-2.7	-2.1	953	T--
Rg	-2.1			-70.1			-8.1			2	-AS

Table 6.4.2. Comparison between REB entry for NPE09 and REB (2001 - 2009) mean and median onset time, backazimuth and slowness residuals for the MKAR array.

phase	NPE09 Tres	REB $Tres_{me}$	REB $Tres_{md}$	NPE09 Bres	REB $Bres_{me}$	REB $Bres_{md}$	NPE09 Sres	REB $Sres_{me}$	REB $Sres_{md}$	REB N	NPE09 problematic
Pn	-0.2	0.4	0.3	3.8	-1.4	-1.2	-2.5	-0.3	-0.3	6890	--s?
Pg	1.4	1.0	0.7	-4.4	1.4	1.8	-4.1	-2.1	-2.0	672	--s?
Sn	3.5	-0.2	0.0	-2.4	1.0	1.1	-11.8	-1.6	-1.0	2049	T-S
Lg	-0.7	-2.2	-1.7	-1.0	2.6	1.6	-4.4	-4.1	-3.6	2755	---

Table 6.4.3. Comparison between REB entry NPE09 and REB (2001 - 2009) mean and median onset time, backazimuth and slowness residuals for the ZALV array.

phase	NPE09 Tres	REB $Tres_{me}$	REB $Tres_{md}$	NPE09 Bres	REB $Bres_{me}$	REB $Bres_{md}$	NPE09 Sres	REB $Sres_{me}$	REB $Sres_{md}$	REB N	NPE09 problematic
Pn	-0.4	-0.1	-0.1	6.7	2.6	2.1	0.5	-0.9	-0.9	1176	---
Sn	16.2	-2.4	-2.2	2.4	1.6	1.3	-3.8	-1.9	-1.6	348	T--
Lg	0.6	2.1	-1.0	-0.7	2.9	1.5	-3.0	-5.9	-5.9	789	---

Table 6.4.4. Comparison between REB entry NPE09 and REB (2001 - 2009) mean and median onset time, backazimuth and slowness residuals for the BVAR array.

phase	NPE09 Tres	REB $Tres_{me}$	REB $Tres_{md}$	NPE09 Bres	REB $Bres_{me}$	REB $Bres_{md}$	NPE09 Sres	REB $Sres_{me}$	REB $Sres_{md}$	REB N	NPE09 problematic
Pn	-0.2	0.9	0.7	3.1	-5.7	-6.1	0.3	-0.1	-0.5	2165	---
Sn	-0.7	0.3	-0.1	-6.6	-3.9	-4.3	-2.3	-1.6	-1.8	863	---
Lg	-3.3	-4.3	-3.6	-0.6	-4.5	-5.3	-1.8	-5.2	-5.3	1064	---

The REB NPE09 solution residuals were plotted together with all reported residuals as function of the epicentral distance (not shown). Whenever an REB NPE09 residual was laying outside the cloud of the other observations, a marker (T for time, A for backazimuth and S for slowness) was used in column "problematic" of the tables above. Lower case characters with question mark (see Table 6.4.2) denote residuals laying at the borders of the observation cloud. In the case of the Rg phase at KURK, only two observations can be found in the entire dataset, so no statistics can be provided. From the tables it becomes clear that several observations at KURK, MKAR and the Sn arrival time at ZALV do not fit the solution satisfactorily. It is evident that these observations need to be reviewed, as they can be the results of either wrong interpretation of readings or insufficiently modelled lateral heterogeneities.

Review of the REB solution

In the light of the above, we first tried relocating the event based solely on the stations used in the REB solution. We have currently no utilities for applying the Source-Specific Station Corrections (SSSCs) used to produce the REB NPE09 solution, so no SSSCs were applied. We tried several global and regional models in our disposal, *i.e*, the global models AK135 (Kennett *et al.*, 1995) and IASP91 (Kennett and Engdahl, 1991), the global 5°x5° model CRUST5.1 (Mooney *et al.*, 1998) and velocity models for the STS region we found in literature (Belyashova *et al.*, 2001; Mikhailova *et al.*, 2002). All data analysis was performed using NORSAR's EP software package, while event location was performed using the HYPOSAT algorithm (Schweitzer, 2001; 2002).

A review of the REB observations made immediately clear the reasons for the large residuals reported in that solution. The worst case was KURK (Table 6.4.1), which is a large, cross-shaped array situated in a distance of approximately 70 km from the event and which is deployed over variable site conditions. Due to the large array aperture, usual plane wave approximation cannot be used for events located so close. In addition, the signals of this event are quite incoherent between farther apart array sites. However, we did attempt array processing by using only a part of the array, with reasonable results. The other obvious problematic case was the Sn phase at ZALV (Table 6.4.3), which is a clear case of phase misidentification and was consequently repicked. Minor changes were made also for other readings, after the application of different filters and the construction of a variety of array beams.

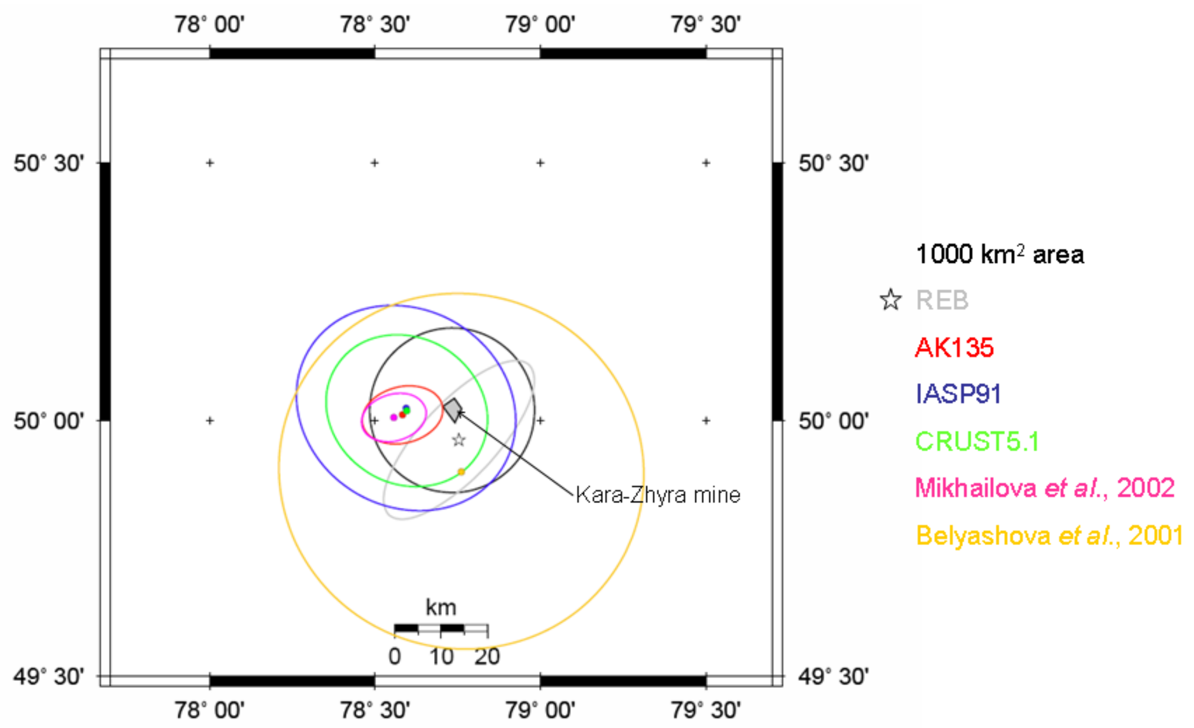

Fig. 6.4.2. Epicenters (circles) and error ellipses for the relocation of the NPE09 event by using only the data appearing in the REB solution. The REB solution (star), the Kara-Zhyra mine (gray polygon) and the 1000 km^2 area (black circle) around the mine are also displayed.

The results of our reanalysis and corresponding location uncertainty in the form of 95% confidence-level error ellipses with the use of the velocity models mentioned above can be seen on the map of Fig. 6.4.2, together with the REB NPE09 location and the approximate location of the Kara-Zhyra mine. All locations correspond to a fixed depth of 0.0 km.

The models fitting the data best are the one based on the travel-time curves calculated by Mikhailova *et al.* (2002) and AK135. With the exception of the solution based on the travel-time curves calculated by Belyashova *et al.* (2001), the rest of our relocations are situated more or less in the same place, but outside the area of the mine, while the "best" solutions have error ellipses that do not include any part of the area occupied by the mine.

Relocation of the NPE09 event with more near-regional data

The next step in our analysis was to try to include in our relocation as many near-regional data as possible, in an attempt to decrease the azimuthal gap in the event location process. Zlata Sinyova of the KNDC kindly provided the full set of array data for the Karatau (KKAR) and the Akbulak (ABKAR) arrays, while KNET station USP, AAK and EKS2 data were retrieved from IRIS (Fig. 6.4.3). Moreover, Pg and Sg onsets were picked for all 20 elements of the KURK array, to be used as a network. Several attempts were made to relocate the event using AK135 and the regional models for the STS region. Among the varying factors were the number of stations used and the definition of the associated phases (e.g., Sn vs Sg/Lg). The final location for the NPE09 event by the use of near-regional data that we are suggesting herein can be seen in Fig. 6.4.4.

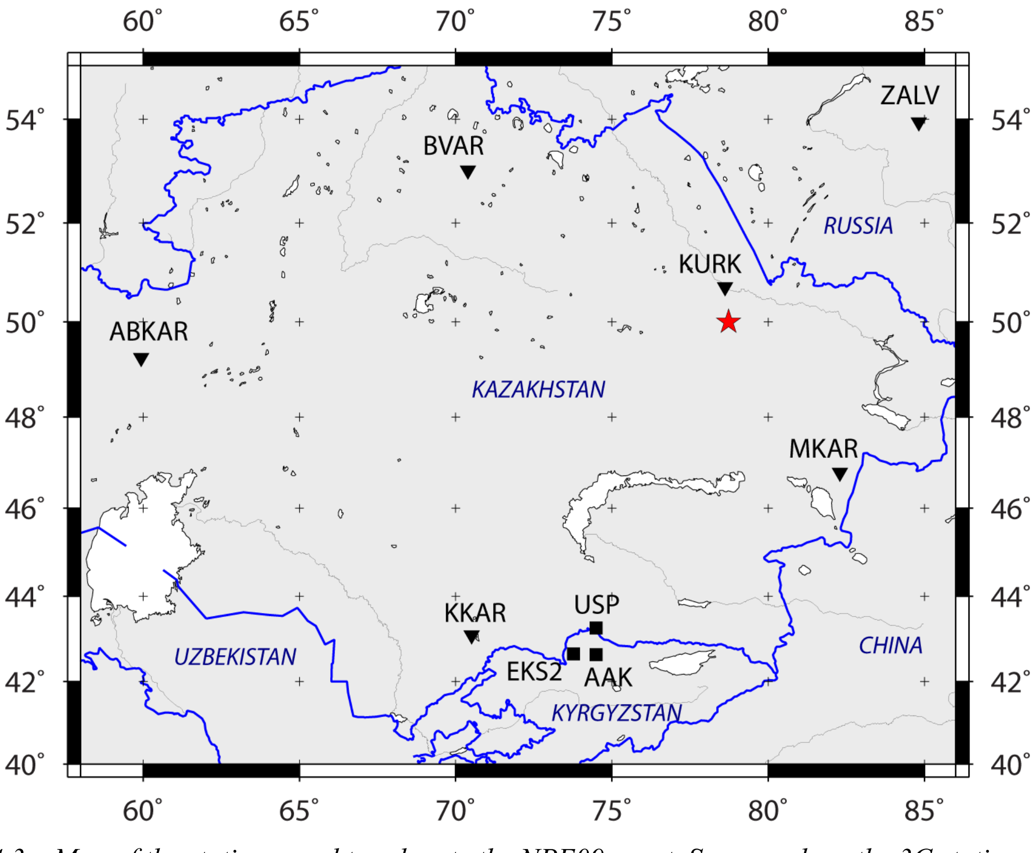

Fig. 6.4.3. Map of the stations used to relocate the NPE09 event. Squares show the 3C stations and inverted triangles the seismic arrays. The source area is located at the red star.

Table 6.4.5. The final solution with the use of near-regional data.

	Parameter value	Uncertainty
Origin time	28/11/2009 07:20:36.868	0.213 s
Latitude	50.0125°N	0.0117°
Longitude	78.6944°E	0.0448°
Depth	0.0 km	Fixed
RMS	0.911 s	
95% error ellipse major semi-axis	2.96 km	
95% error ellipse minor semi-axis	1.13 km	
95% error ellipse azimuth	89.1°	
95% error ellipse area	10.5 km^2	
N of defining observations	8	
N of defining onset times	55	
Maximum azimuthal gap	100.9°	
Velocity model	Mikhailova *et al.*, 2002	

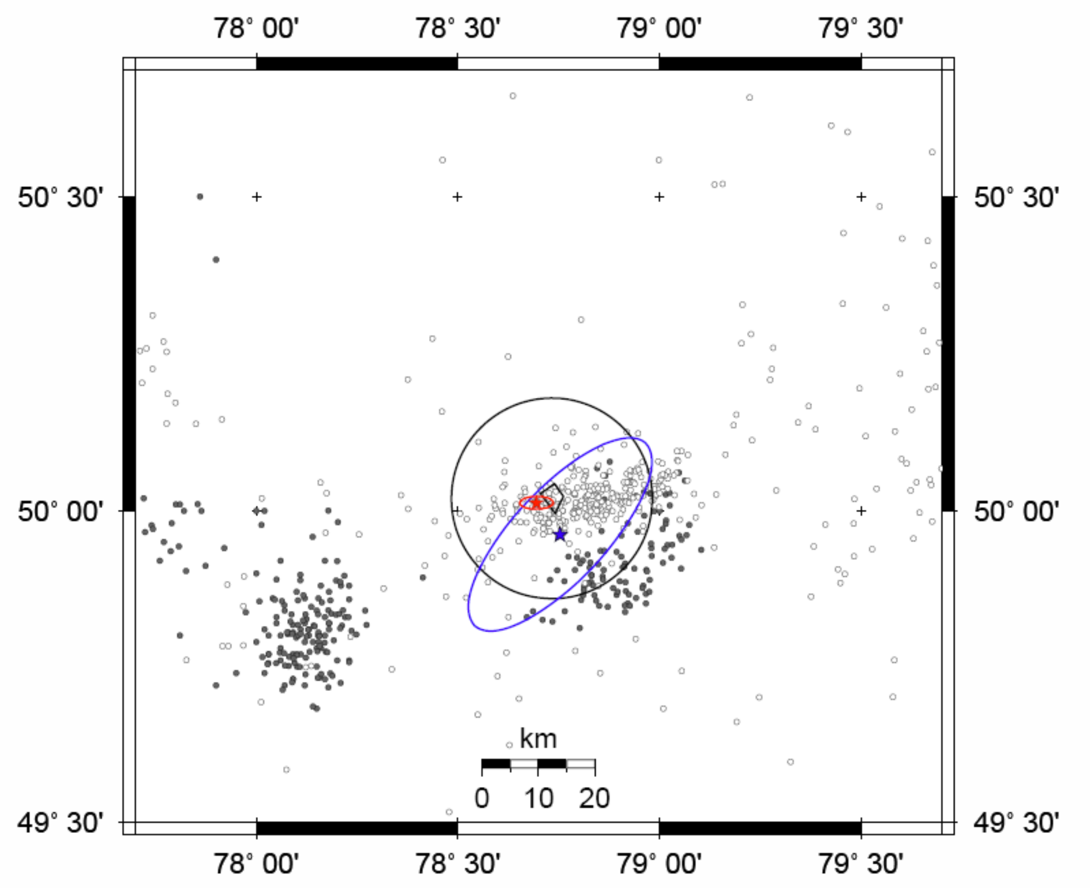

Fig. 6.4.4. Our final relocation of the NPE09 event (red star), the REB solution (blue star) and corresponding 95% confidence level error ellipses. The location of the Kara-Zhyra mine (polygon) and an area of 1000 km^2 around it, as well as the locations of the seismic events in the ISC On-line Bulletin (ISC, 2001) are displayed. Filled circles are ISC events prior to 1991, when testing was being conducted at Balapan, while open circles are events after 1991 and presumably correspond mainly to mining activity.

Table 6.4.6. Event location input data and corresponding residuals.

station	dist (°)	azi (°)	phase	onset time	res	used
KUR10	0.539	344.27	Pg	07:20:46.422	-0.661	T--D
KUR10	0.539	344.27	Sg	07:20:55.300	1.232	T--D
KUR09	0.556	345.24	Pg	07:20:46.771	-0.628	T--D
KUR09	0.556	345.24	Sg	07:20:55.613	1.003	T--D
KUR08	0.574	346.13	Pg	07:20:47.119	-0.625	T--D
KUR08	0.574	346.13	Sg	07:20:55.779	0.576	T--D
KUR07	0.592	346.96	Pg	07:20:47.495	-0.580	T--D
KUR07	0.592	346.96	Sg	07:20:56.482	0.712	T--D
KUR11	0.597	357.53	Pg	07:20:47.477	-0.752	T--D
KUR11	0.597	357.53	Sg	07:20:55.784	-0.251	T--D
KUR12	0.602	355.64	Pg	07:20:47.696	-0.608	T--D
KUR12	0.602	355.64	Sg	07:20:56.075	-0.089	T--D
KUR13	0.608	353.87	Pg	07:20:47.745	-0.656	T--D
KUR13	0.608	353.87	Sg	07:20:56.163	-0.176	T--D
KUR06	0.614	347.81	Pg	07:20:47.826	-0.648	T--D
KUR06	0.614	347.81	Sg	07:20:56.459	0.004	T--D
KUR14	0.615	352.06	Pg	07:20:47.925	-0.594	T--D
KUR14	0.615	352.06	Sg	07:20:56.477	-0.056	T--D
KUR15	0.622	350.27	Pg	07:20:48.048	-0.578	T--D
KUR15	0.622	350.27	Sg	07:20:56.273	-0.443	T--D
KUR16	0.639	346.89	Pg	07:20:48.195	-0.717	T--D
KUR16	0.639	346.89	Sg	07:20:57.527	0.320	T--D
KUR05	0.649	349.26	Pg	07:20:48.417	-0.691	T--D
KUR05	0.649	349.26	Sg	07:20:57.402	-0.141	T--D
KUR17	0.649	345.31	Pg	07:20:48.371	-0.723	T--D
KUR17	0.649	345.31	Sg	07:20:57.589	0.070	T--D
KUR18	0.656	343.76	Pg	07:20:48.425	-0.779	T--D
KUR18	0.656	343.76	Sg	07:20:58.993	1.284	T--D
KUR19	0.666	342.14	Pg	07:20:48.570	-0.820	T--D
KUR19	0.666	342.14	Sg	07:20:58.475	0.448	T--D
KUR04	0.667	349.93	Pg	07:20:48.775	-0.674	T--D
KUR04	0.667	349.93	Sg	07:20:58.159	0.029	T--D
KUR20	0.677	340.68	Pg	07:20:48.649	-0.925	T--D
KUR20	0.677	340.68	Sg	07:21:01.263	2.920	T--D
KUR03	0.685	350.43	Pg	07:20:49.176	-0.598	T--D
KUR03	0.685	350.43	Sg	07:20:58.931	0.245	T--D
KUR02	0.705	351.17	Pg	07:20:49.649	-0.491	T--D
KUR02	0.705	351.17	Sg	07:20:59.528	0.214	T--D
KUR01	0.723	351.71	Pg	07:20:50.071	-0.410	T--D
KUR01	0.723	351.71	Sg	07:21:00.116	0.215	T--D
MKAR	3.996	142.20	Pn	07:21:40.650	0.291	T--D
MKAR	3.996	142.20	Pg	07:21:48.886	-1.213	T--D
MKAR	3.996	142.20	Sn	07:22:30.337	1.779	T--D
MKAR	3.996	142.20	Sg	07:22:43.496	0.734	T--D
ZALV	5.454	41.30	Pn	07:22:01.013	1.461	T--D
ZALV	5.454	41.30	Sn	07:23:00.608	-2.269	T--D
BVAR	6.018	303.34	Pn	07:22:08.269	1.572	T--D
BVAR	6.018	303.34	Sn	07:23:16.136	0.508	T--D
USP	7.341	204.92	Pn	07:22:25.216	0.608	T--D
USP	7.341	204.92	Sn	07:23:47.417	-0.184	T--D
AAK	7.928	203.26	Pn	07:22:32.218	-0.377	T---
EKS2	8.103	206.84	Pn	07:22:33.980	-0.869	T---
KKAR	8.923	222.43	Pn	07:22:45.317	-0.192	T--D
KKAR	8.923	222.43	Sn	07:24:27.170	2.219	T--D
ABKAR	12.205	273.67	Pn	07:23:29.779	0.967	T---

The focal parameters, corresponding uncertainties and general information about the final NPE09 solution suggested in this contribution are summarized in Table 6.4.5. Phase information, input parameter values, corresponding residuals and information about defining observations can be found in Table 6.4.6.

The velocity model based on the travel-time curves by Mikhailova *et al.* (2002) used up to a distance of 13° and thus covering all employed stations, is the one that provides in general the best fit to the available data. However, S-phases and especially Lg are not modelled satisfactorily at all distances. For distances up to 5°, modelling the high amplitude S-phase as Sg provides the best fit, while for larger distances residuals are smaller if the phase is identified as Lg. HYPOSAT cannot extract an Lg velocity from an applied velocity model, but an Lg group velocity value can be assigned through the parameter file (Schweitzer, 2002). The group velocity value of 3.54 km/s, which corresponds to the travel-time curves calculated by Mikhailova *et al.* (2002), produces rather high residuals. Taking these into consideration, we decided to treat the S-phase readings as Sg up to about 5° and as Lg for the rest of the stations, without including the latter in the location process. All other available onset readings were used. In addition, whenever more than one onset reading from the same station was available, we also inverted for the travel-time differnce between these onsets. Such cases are indicated with a "D" in Table 6.4.6. In our final inversion we did not use any slowness vector observation since they are in this case (source - station geometry) of little importance to the solution.

The final solution shows some quite large travel-time residuals at some stations (for P or S onsets). These residuals might be caused by insufficient modelling of lateral heterogeneities by a simple horizontally layered velocity model. Reports can be found in literature (see *e.g.*, Ringdal et al., 1992; Bonner *et al.*, 2001 and references therein) of two distinct shear-wave velocity zones at the Balapan Test Site, a relatively high velocity area to the SW and a lower velocity area to the NE, their NW-SE trending boundary roughly coinciding with the Chinrau fault. Such information, combined with observed contrasts in Lg amplitudes and spectral and waveform differences for teleseismic P-phases between the NE and SW regions of the Balapan Test Site are highly suggestive of structural complexities that are presumably unaccounted for by the velocity model.

6.4.3 Concluding remarks

The NDC Preparedness Exercise 2009 event was relocated with the use of near-regional seismic data. The suggested location is in good agreement with the information we have about the nature of the event, namely that it corresponds to a mining explosion in the Western Kara-Zhyra open pit mine.

The process of relocating the NPE09 event revealed several interesting aspects of possible path and structure interference in earthquake location and highlighted the importance of the availability of appropriate velocity models and SSSCs, in particular within the CTBTO monitoring framework.

Myrto Pirli

Johannes Schweitzer

Acknowledgements

Zlata Sinyova of the KNDC kindly provided the data from the KKAR and ABKAR arrays, as well as a great wealth of information on the event and velocity models for the region. KNET station data were retrieved from IRIS (http://www.iris.edu/data/).

References

Belyashova, N.N., V.I. Shacilov, N.N. Mikhailova, I.I. Komarov, Z.I. Sinyova, A.V. Belyashov & M.N. Malakhova (2001). On the use of calibration explosions at the former Semipalatinsk Test Site for compiling a travel-time model of the crust and upper mantle. Pure Appl. Geophys. **158**, 193-209.

Bonner, J.L., C.D. Pearson, S.W. Phillips & S.R. Taylor (2001). Shallow velocity structure at the Shagan River Test Site in Kazakhstan. Pure Appl. Geophys. **158**, 2017-2039.

ISC (2001). On-line Bulletin, http://www.isc.ac.uk, Internatl. Seis. Cent., Thatcham, United Kingdom.

Kennett, B.L.N. & E.R. Engdahl (1991). Travel times for global earthquake location and phase identification. Geophys. J. Int. **105**, 429-465.

Kennett, B.L.N., E.R. Engdahl & R. Buland (1995). Constraints of seismic velocities in the Earth from travel times. Geophys. J. Int. **122**, 108-124.

Михайлова Н.Н., И.Л. Аристова и Т.И. Германова (2002). Годограф сейсмических волн по результатам регистрации сигналов от химических взрывов на Семипалатинском испытательном полигоне. Вестник НЯЦ РК **выпуск 2**, **сентябрь 2002**, 46-54. (Mikhailova, N.N., I.L. Aristova & T.I. Germanova (2002). Seismic waves travel-time curve basing on the results of signal detection from chemical explosions detonated at Semipalatinsk Test Site. Bull. NNC RK **Release 2**, **September 2002**, 46-54.)

Mooney, W.D., G. Laske & G. Masters (1998). CRUST5.1: A global crustal model at 5°x5°. J. Geophys. Res. **103**, 727-747.

Ringdal, F., P.D. Marshall & R.W. Alewine (1992). Seismic yield determination of Soviet underground nuclear explosions at the Shagan River test site. Geophys. J. Int., **109**, 65-77.

Schweitzer, J. (2001). HYPOSAT – An enhanced routine to locate seismic events. Pure Appl. Geophys. **158**, 277-279.

Schweitzer, J. (2002). PD11.1: User Manual for HYPOSAT (including HYPOMOD). In: Bormann, P. (Ed.) (2002). IASPEI New Manual of Seismological Observatory Practice, GeoForschungsZentrum Potsdam, Vol. 2, 15 pp.